Examination of Assumptions for Local Cerebral Blood Flow Studies in PET

Robert A. Koeppe, Gary D. Hutchins, Jill M. Rothley, and Richard D. Hichwa

Cyclotron/P.E.T. Facility, Division of Nuclear Medicine, Department of Internal Medicine, University of Michigan Medical School, Ann Arbor, Michigan

Two common assumptions made in most positron emission tomography (PET) cerebral blood flow techniques have been examined in detail. These are (1) that the blood-borne radioactivity component in the measured PET data is negligible, and (2) that differences in arrival time of the arterial bolus across the brain cause insignificant biases in the estimated cerebral blood flow (CBF) values. Biases in CBF values due to partial failure of these assumptions have been predicted by computer simulation studies and also quantitated for both dynamic and single scan PET methods using $H_2{}^{15}O$. Both computer simulations and measured PET data indicate that these assumptions can sometimes cause significant errors in the estimated flow values. The magnitude of these errors depends on the PET technique used (dynamic or static) and on the interval of data included in the flow calculations. The bias caused when these assumptions fail can be considerably reduced by omitting ~40 sec of data immediately following tracer administration from the CBF calculations.

J Nucl Med 28:1695–1703, 1987

Positron emission tomography (PET), together with the use of inert freely diffusible radioindicators, can provide quantitative measurements of local cerebral blood flow (CBF). Examples of positron-emitting radioindicators for estimating CBF include oxygen-15 (^{15}O) water or [^{15}O]carbon dioxide (*1–5*), fluorine-18 (^{18}F) fluoromethane (*6,7*), carbon-11- and [^{15}O]butanol (*8,9*), and krypton-77 (*10*). The accuracy of the estimated CBF values is dependent on (a) the statistical precision of the measured data (both PET and arterial input function) and (b) the validity of assumptions made in the kinetic model and in the parameter estimation scheme used to calculate CBF. In this report we examine the second of these two factors.

At least six assumptions exist that, if not completely valid, will introduce bias into the blood flow estimates. These are: (a) the CBF tracer equilibrates instantaneously between blood and brain tissue and, therefore, the blood-borne radioactivity component of the measured PET data is negligible; (b) differences in arrival time of the arterial bolus across the brain are insignificant; (c) a single fixed value of the tissue-blood partition coefficient of water may be used for the entire brain (static methods only); (d) the measured arterial input curve from the radial artery and the true arterial input to the brain have the same shape; (e) each individual region is homogeneous with respect to flow and partition coefficient; and (f) a two-compartment model configuration (blood and a single tissue compartment) governed by two rate constants accurately describes the true in vivo behavior of the radioindicator. If these assumptions are valid, then the estimates of CBF should be unbiased and independent of the temporal range of PET data used in the calculation. However, the occurrence of varying CBF estimates with different PET scan time ranges indicates that one or more of the assumptions is not entirely valid. This work focuses on the first two of these six assumptions. The final four assumptions in the above list have been investigated and reported by others (*11–15*).

We will first briefly review the model equations for CBF PET studies and describe how more careful consideration of the above assumptions affects the equations describing kinetic behavior. We then present results from computer simulation studies performed to determine the magnitude of the biases encountered during typical CBF studies. We also present results of measured PET data acquired following intravenous bolus administration of $H_2{}^{15}O$. Finally, we discuss the conditions under which failure of these assumptions causes significant bias in estimated CBF values and describe methods to minimize these sources of error.

Received Oct. 6, 1986; revision accepted May 28, 1987.

For reprints contact: Robert A. Koeppe, PhD, Cyclotron/P.E.T. Facility, University of Michigan Medical School, 3480 Kresge III, Box 0552, Ann Arbor, MI 48109-0552.

THEORY

The solution to the Kety-Schmidt blood flow model is commonly written as:

$$C_t(t) = fC_a(t) \otimes e^{-[(f/p)+\lambda]t}, \quad (1)$$

where $C_t(t)$ and $C_a(t)$ are the time varying radioactivity concentrations (μCi/ml) in tissue and arterial blood, respectively, f is the local mass specific blood flow (ml of blood/ml of brain/ min), p is the tissue-blood partition coefficient for H_2O (ml of blood/ml of brain), λ is the decay constant for ^{15}O (1/min), and $\otimes$ represents mathematic convolution.

Even though complete equilibration between tissue and blood occurs during a single capillary transit for a freely diffusible tracer, the arterial blood remains at a different concentration than brain tissue. The early PET data will have considerable contributions from arterial-borne radioactivity and thus CBF estimates will be biased when blood corrections are not made. When the tracer rapidly equilibrates between blood and tissue and when the tissue-blood partition coefficient of the water is near unity (so venous and tissue concentrations are approximately equal), the blood volume component can be approximated by the cerebral blood volume (CBV), given in ml of blood/ml of brain, multiplied by the arterial fraction of the total CBV (F_a). The measured PET data ($C_{PET}(t)$) as a function of time becomes:

$$C_{PET}(t) = (1 - CBV\ F_a)[fC_a(t) \otimes e^{-[(f/p)+\lambda]t}] + CBV\ F_a\ C_a(t). \quad (2)$$

Note that f now actually represents perfusion of the brain exclusive of the arterial vascular space and p represents the effective partition coefficient between brain (exclusive of the arterial vascular space) and blood. However, even if the venous blood volume is 5% of the tissue volume and the true partition coefficient of water differs from unity by 20%, only a 1% error in either f or p would result.

Due to differences in the lengths and diameters of separate branches of the cerebral vasculature, there exist variations in the arrival time of the radioactivity bolus to local regions of the brain. These can be accounted for by variable temporal shifts of the measured arterial input curve (at the radial artery) with respect to the PET data sequence of each individual brain tissue region. Thus, Eq. (2) can be rewritten as:

$$C_{PET_i}(t) = (1 - CBV\ F_a)[fC_a(t - t_i) \otimes e^{-[(f/p)+\lambda]t}] + CBV\ F_a\ C_a(t - t_i). \quad (3)$$

The arterial input C_a is now a function of t_i, which describes the variable temporal shift of the measured arterial curve with respect to the measured tissue curve for each region i.

PET CBF techniques that use inert freely diffusible radioindicators can be categorized into three groups: (a) steady-state methods (*4,5*); (b) autoradiographic methods (*2,3,19*); and (c) dynamic methods (*1,6,7,10*). All studies reported in this work were performed using a bolus administration and, thus, only the autoradiographic and dynamic methods were investigated. The effects of errors caused by violations of the assumptions investigated in our study are considerably different for steady-state methods than for bolus administration methods and, therefore, will not be discussed further in this paper.

Dynamic methods estimate both flow and the tissue-blood partition coefficient, while single scan methods estimate only flow and therefore must assume a fixed and, for practical implementation, a uniform value of the partition coefficient. The dynamic analysis was performed using a weighted integral lookup table technique (*18*). The computational form of the method appears as:

$$\frac{\int_{T_1}^{T_2} w_1(t)C_t(t)\,dt}{\int_{T_1}^{T_2} w_2(t)C_t(t)\,dt} = \frac{f\int_{T_1}^{T_2} w_1(t)C_a(t) \otimes e^{-[(f/p)+\lambda]t}\,dt}{f\int_{T_1}^{T_2} w_2(t)C_a(t) \otimes e^{-[(f/p)+\lambda]t}\,dt}, \quad (4)$$

where $w_1(t)$ and $w_2(t)$ are time-dependent weighting functions. The weighting functions used in this work were $w_1(t) = 1/\sqrt{t}$ and $w_2(t) = \sqrt{t}$. The leading f terms on the right side cancel and f/p can be estimated by comparing measured data (left side) to a calculated lookup table involving the arterial input function and f/p (right side). Once f/p has been estimated f is easily obtained by substituting f/p back into the integral equation. Finally an estimate of p is obtained by dividing the estimate of f by the estimate of f/p. Our selection of weighting functions differs from that of 1 and t chosen in the original description of the method (*18*). Simulation studies show slightly superior performance for the weighting function pair of $1/\sqrt{t}$ and $\sqrt{t}$ compared with 1 and t in terms of reducing both bias and uncertainty in the parameter estimates. This rapid analysis technique has also been shown to perform nearly as well as standard nonlinear least-squares techniques, but with dramatic improvement in computation time (*15*).

The single scan analysis was performed using a fixed value for the tissue-blood partition coefficient, allowing the measured PET value to be written as a function of only one unknown parameter f.

$$\int_{T_1}^{T_2} C_t(t)\,dt = f\int_{T_1}^{T_2} C_a(t) \otimes e^{-[(f/p)+\lambda]t}\,dt. \quad (5)$$

Blood flow is then easily calculated using either a lookup table or an analytic relationship between the left and right side of Eq. (5).

METHODS

Theoretical computer simulation studies were performed to predict the biases encountered in estimated CBF values caused by the arterial-borne radioactivity component of the PET data. Simulated noise-free PET data were calculated using the model equations [Eq. (1)] with the arterial input function shown in Figure 1. Gray and white matter regions are assumed to have blood flow values of 70 and 20 ml/100 ml/min, respectively. An arterial blood volume component was added to the noise-free data according to Eq. (2). Blood flow values were then estimated without accounting for the blood-borne component by using either Eqs. (4) or (5). CBF values were estimated in a total of five ways using the two different estimation techniques. The dynamic two-parameter analysis was performed using either 4 min or 6 min of data. The single scan analysis was performed using 40 sec, 100 sec, or 240 sec of data. Longer data acquisition intervals provide more total coincidence counts and therefore higher statistical accuracy. However, the later data becomes less dependent on

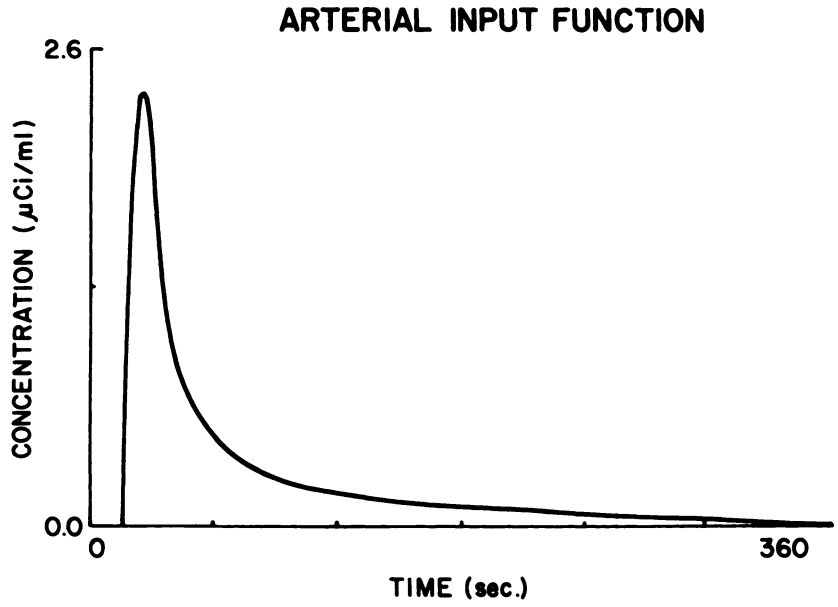

FIGURE 1
Measured arterial input function time course as measured from the radial artery following intravenous bolus injection of ^{15}O-H_2O. This input curve was used for all theoretical computer simulations.

flow while becoming more dependent on the partition coefficient.

Equation 3 was used to predict changes in the estimated CBF values caused by variations in the arrival time of the arterial bolus across the brain. Simulated PET data was calculated using Eq. (1). Again, gray and white matter regions were assumed to have blood flow values of 70 and 20 ml/100 ml/min, respectively. CBF values were estimated using either Eqs. (4) or (5), but with the arterial input function shifted 3 sec either forward or backward in time.

Measured PET data was acquired on a TCC PCT-4600A tomograph, with in-plane resolution of ~10.5–11.0 mm full width at half maximum (FWHM) and axial resolution of ~10.0 mm FWHM. Blood flow studies were performed on three normal volunteer subjects using an intravenous bolus injection of 25–30 mCi of $H_2{}^{15}O$. PET scanning was always initiated at the start of injection. A dynamic sequence of scans was acquired as follows; six scans of 20 sec duration, two scans of 1 min duration, and one scan of 2 min duration, totaling nine scans in 6 min. The arterial blood concentration was recorded continuously from the radial artery using a flow through plastic scintillation detector (*20*). The detector was placed ~8 cm from the tip of the catheter and blood was withdrawn at a rate of 5.0 ml/min. The mean head to radial artery arrival time difference used for timing of the measured input function was determined by recording the total coincidence events from the middle ring of the scanner at 1-sec intervals and matching the leading edge of this curve to the leading edge of the input curve measured at the radial artery. The dynamic analysis was then performed by the weighted integral lookup table method [Eq. (4)] using either the first eight scans (4 min) or all nine scans (6 min). The single scan analysis [Eq. (5)] was performed by summing data from three scans (60 sec), five scans (100 sec), or eight scans (240 sec) into a single data set. All values reported without the first 40 sec of data were obtained simply by omitting the first two scans of the dynamic sequence from all calculations.

Estimates of the arrival time difference between a brain region and the measured arterial input function were obtained by fitting the arrival time differential as an additional parameter in the model, instead of using a fixed mean value for the arrival time as described in the preceding paragraph. The input function, recorded on a 1-sec time grid by the flow through detector, was linearly interpolated to allow fractional displacements of the input curve. Arrival time, CBF, and p were simultaneously estimated by standard nonlinear least-squares analysis. Calculations were made using the entire 6-min dynamic sequence of PET data.

RESULTS

Theoretical effects of arterial blood volume on estimated CBF values are described in Figure 2. Shown are percent overestimations in CBF as a function of arterial blood volume. Estimation of both blood flow and partition coefficient was performed using the dynamic information from 4 min or 6 min of data. Single scan analyses were performed using an assumed partition coefficient of 0.9 ml of blood/ml of brain and data intervals of 60 sec, 100 sec, or 240 sec. The two left panels show results when the data immediately following bolus injection of tracer is included in the calculation. The two right panels show results when the first 40 sec of data are excluded.

Table 1 summarizes the computer simulation studies showing the effect of including the first 40 sec of data following tracer administration in the estimation procedure. These values are obtained by comparison of the left and right panels in Figure 2. Given are the percent increases in CBF when the estimation includes the first 40 sec of data. Results for three arterial blood volume fractions are shown; 0.1 (near a major artery), 0.02 (high gray matter region), and 0.005 (typical white matter region).

Functional images of CBF at two levels of the brain

FIGURE 2
Theoretical effects of arterial blood volume on estimated CBF values. Shown are percent overestimations in CBF as a function of arterial blood volume fraction. A dynamic technique, estimating both blood flow and partition coefficient, was performed using both 4 min or 6 min of data. A single scan technique, using an assumed partition coefficient, was performed using 40 sec, 100 sec, or 240 sec of data. The two left panels show results when the data immediately following bolus injection of tracer is included in the calculation. The early PET data can have significant blood contributions even if the arterial blood volume fraction is only 1% or 2%, resulting in overestimations in CBF. The two right panels show results when the first 40 sec of data are excluded. The CBF overestimations are considerably smaller.

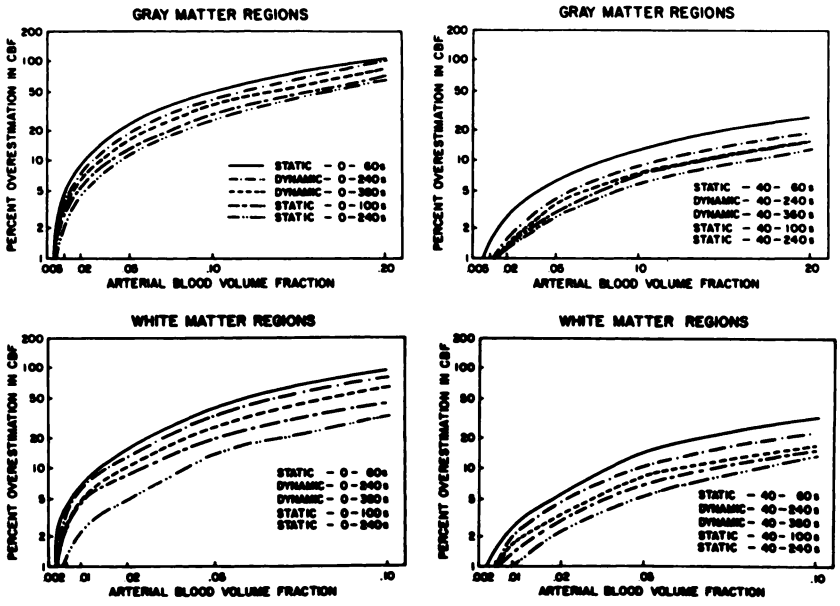

for one control subject are shown in Figure 3. Each brain level was analyzed with (top images) and without (bottom images) the first 40 sec of PET data. A dynamic analysis using 6 min of data was employed for these calculations. Note the obvious effect of blood-borne radioactivity on the estimated flow values in the regions surrounding the carotid arteries when the early data is included. Excluding the first 40 sec of data alleviates much of this effect. Boundaries of typical regions of interest (ROIs) for areas surrounding major arterial vessels and for areas composed primarily of temporal lobe gray matter, cerebellar white matter, and parietal white matter are pictured in Figure 4. Similar sets of ROIs were drawn for each subject.

Table 2 summarizes the measured percent differences in estimated CBF with and without the first 40 sec of data. Positive values indicate higher estimates when the first 40 sec of data is included. The means and standard deviations were obtained from several regions on three different subjects; arterial (n = 6), temporal (n = 8), and white matter (n = 10). Each of the five rows represents a different analysis of the same set of studies. The measured results reported in this table compare well with the theoretical predictions shown in Table 1.

Table 3 reports both theoretical and experimentally measured changes in estimated CBF due to regional differences in the arrival time of the arterial blood to various regions of the brain. Three-second variations in arrival time were simulated for several data acquisition intervals for both the dynamic and static analysis methods. A positive time shift indicates a larger time difference between measured and actual arterial input functions. The experimentally measured results are derived from the same data reported in Table 2. Table values are the mean change in CBF for gray and white matter regions when the arrival of the arterial input function is shifted in time. It can be seen that theoretical CBF changes due to arrival time variations are in good agreement with those changes seen in experimentally measured data.

Table 4 presents the estimated arrival time differentials between various brain regions and the measured arterial input function when the arrival time is included as a third model parameter for one of the subjects reported in Tables 2 and 3. In addition, Table 4 compares CBF values for estimated and fixed mean arrival times, where the value of the fixed mean arrival time is calculated as described in the Methods section. The top two rows give the mean and standard deviation of the estimated time differential (in seconds) between arrival of radioactivity in the brain region and the radial artery.

TABLE 1
Theoretical Effect of the First 40 sec of PET Data on Estimated CBF*

Scan duration (sec)	Arterial blood volume fraction		
	0.1	0.02	0.005
Dynamic			
240 sec	65.4	7.1	2.5
360 sec	51.9	6.4	2.1
Static			
60 sec	60.0	6.5	2.0
100 sec	33.8	4.6	1.0
240 sec	20.3	2.6	0.4

*Table values give predicted percent differences in estimated CBF with and without inclusion of the first 40 sec of data following tracer administration. A positive result indicates higher estimated CBF when the first 40 sec of data is used. These values were obtained by comparing left and right panels of Figure 2.

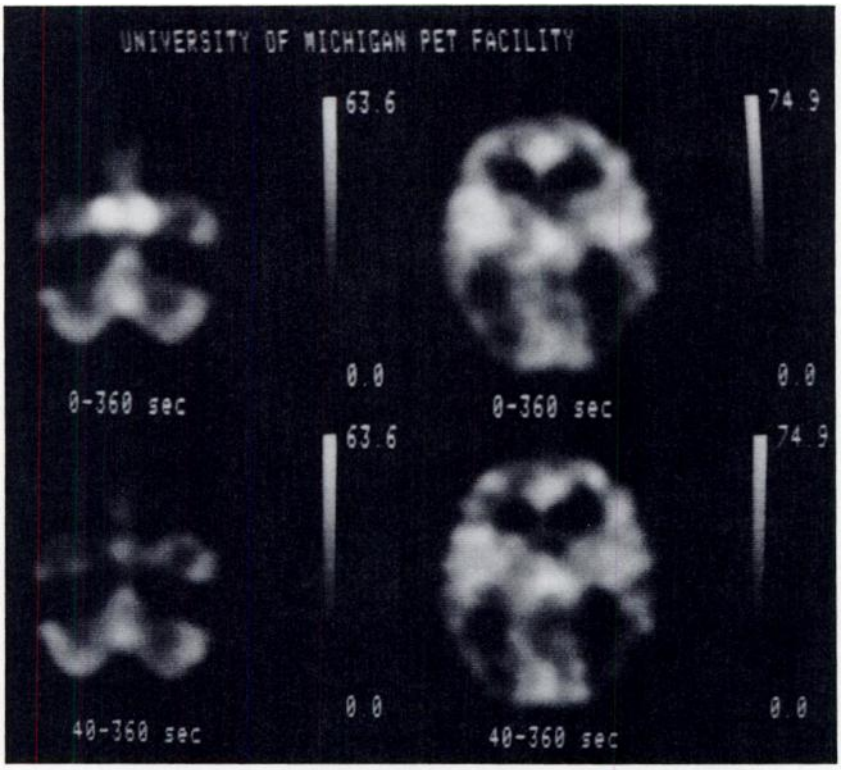

FIGURE 3
Functional images of local cerebral blood flow for one subject. Shown are two levels of the brain acquired from a single administration, each analyzed with (top) and without (bottom) the first 40 sec of PET data. A dynamic analysis using data through 6 min postadministration was employed for each calculation. Note the obvious effect of blood-borne radioactivity on the estimated flow values in the regions surrounding the carotid arteries. Omitting the first 40 sec of data alleviates much of this effect. Decreases in the estimated flow in temporal lobe regions can also be observed when the first 40 sec of data are omitted.

The third row gives the time differential between the estimated arrival time and the fixed mean arrival time of 11 sec for this subject. The fourth and fifth rows give estimated CBF values using measured and then a fixed constant arrival time, respectively. The final row gives the percent change in estimated CBF when the arrival time is fixed to a mean value instead of being estimated as an additional parameter. These results are very similar to results from the other subjects analyzed in this manner.

DISCUSSION

There are many factors involved in the accurate measurement of CBF with PET. Several groups have carefully investigated CBF methods, analyzing the performance and potential sources of error in each measurement technique. An indication that one or more of the assumptions of a blood flow technique may not be entirely valid is the presence of variable CBF estimates as the temporal range of PET data included in the measurement is altered. Raichle (*3*), Ginsberg (*21*), Iida (*12*), and co-workers at their respective laboratories have seen this effect for autoradiographic CBF techniques. Huang et al. (*13*) have observed similar effects in dynamic CBF techniques. Several sources of error causing time-dependent CBF measurements were isolated and analyzed in these studies. They include (a) tissue inhomogeneities, (b) uncertainty in the partition coefficient, (c) dispersion of the measured input function, (d) time shifts between blood and tissue data, and (e) validity of a single compartment model.

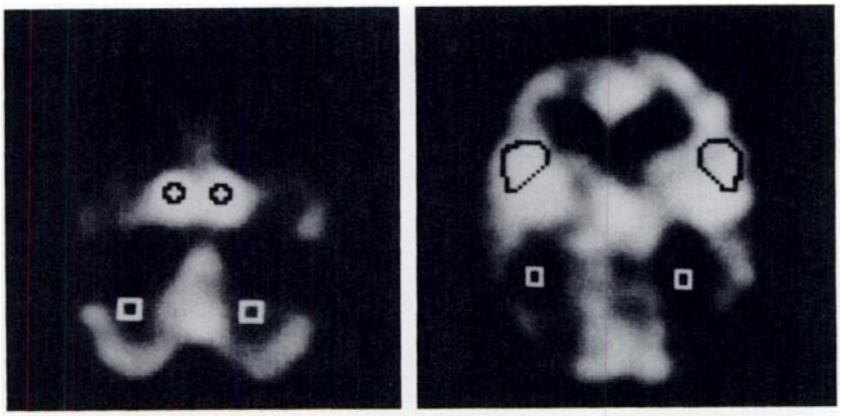

FIGURE 4
Images showing typical regions of interest (ROIs) for areas surrounding the carotid arteries, temporal lobe, and white matter areas. A similar set of ROIs was drawn for each subject.

TABLE 2
Measured Effect of the First 40 sec of PET Data on Estimated CBF*

Scan duration (sec)	Arterial Mean ± s.d.	Temporal Mean ± s.d.	White matter Mean ± s.d.
Dynamic			
240 sec	75.2 ± 30.9	11.8 ± 6.1	1.7 ± 7.6
360 sec	65.9 ± 28.4	11.1 ± 6.1	2.6 ± 6.2
Static			
60 sec	59.1 ± 18.5	8.0 ± 4.2	0.3 ± 7.1
100 sec	37.0 ± 11.5	5.6 ± 2.8	1.1 ± 4.3
240 sec	26.0 ± 9.1	3.0 ± 2.5	1.4 ± 3.2

* Table values give measured percent differences in estimated CBF with and without inclusion of the first 40 sec of PET data. A positive result indicates higher estimated CBF when the first 40 sec of data is used. Means and standard deviations are obtained from several regions from studies performed on three different subjects; arterial (n = 6), temporal (n = 8), and white matter (n = 10). Each of the five rows represents a different analysis of the same studies.

The present work examines two other common assumptions made in both dynamic and single scan CBF techniques that can cause error in the estimated flow, resulting in temporally varying CBF values. These are (a) that the blood-borne radioactivity component in the measured PET data is negligible and (b) that differences in arrival time of the arterial bolus across the brain are insignificant. The effects observed when the first of these assumptions is not entirely valid has not, to our knowledge, been reported previously. If the second assumption is invalid, similar effects to those caused by incorrect time shifts between blood and tissue data are observed. Both result in error caused by the measured blood curve not being appropriately shifted in time relative to the brain data. Previous work has described this effect only for the autoradiographic method and only with inclusion of the early data following administration. The present study reports effects not only for these conditions but (a) when some early data is excluded from the CBF calculations (Table 3), (b) for dynamic CBF estimates (Table 3), and (c) for regional variations in arrival time of the bolus input that a single shift between the blood curve and the mean tissue curve cannot account for (Table 4).

TABLE 3
Percent Change in Estimated CBF due to Regional Arterial Arrival Time Differences*

Scan duration (sec)	Time diff.	Theoretical Gray	Theoretical White	Experimental Gray	Experimental White
Dynamic					
0–240 sec	+3 sec	10.4	8.0	11.9	11.6
	−3 sec	−9.2	−7.8	−10.8	−9.1
40–240 sec	+3 sec	−0.1	1.3	0.6	1.5
	−3 sec	0.2	−1.3	−0.3	−1.4
0–360 sec	+3 sec	8.8	6.1	10.5	8.7
	−3 sec	−7.9	−5.5	−9.6	−7.5
40–360 sec	+3 sec	−0.6	0.6	0.3	1.3
	−3 sec	0.8	−1.1	−0.2	−1.3
Static					
0–60 sec	+3 sec	12.5	11.3	11.3	12.0
	−3 sec	−10.4	−10.0	−9.5	−9.8
40–60 sec	+3 sec	1.1	2.5	0.8	2.1
	−3 sec	−0.4	−2.5	−0.2	−1.6
0–240 sec	+3 sec	1.1	1.3	1.4	1.7
	−3 sec	−1.4	−1.3	−1.2	−1.7
40–240 sec	+3 sec	−5.7	−1.2	−4.2	−1.6
	−3 sec	7.5	1.2	5.5	1.8

* Table values give percent change in estimated CBF when the measured arterial input function is shifted +3 (later in time) and −3 (earlier in time) seconds relative to the PET data. Theoretical computer simulations and measured experimental results are given for both dynamic and static scan techniques.

TABLE 4
Regional Estimates of Arrival Times of the Arterial Input Bolus and Effects on CBF

	Arterial Left	Arterial Right	Temporal Left	Temporal Right	White matter Left	White matter Right
Regional arrival time (relative to radial artery) Mean (sec)	15.2	14.0	10.2	10.8	8.7	9.6
± s.d.	±0.7	±1.2	±0.6	±0.8	±1.1	±1.8
Arrival time difference (s) (estimated—fixed)	4.2	3.0	−0.8	−0.2	−2.3	−1.4
CBF (ml/100 ml/min) (estimated arrival)	37.2	39.8	48.4	49.5	19.3	21.9
CBF (ml/100 ml/min) (fixed arrival = 11 sec)	46.1	46.9	47.2	48.5	18.1	20.8
% Change in CBF	23.9	17.9	−2.5	−2.0	−6.5	−5.3

* The top two rows give the calculated time differential (in seconds) between regional arrival of radioactivity in the brain and the radial artery (the site of arterial input function measurement). Values are the mean and standard deviation of pixels within each region. The third row gives the time difference between the estimated regional arrival time and the fixed mean arrival time (11 sec for this subject). The next two rows give estimated CBF values using both the measured arrival time and the standard fixed arrival time. The bottom row gives the percent change in CBF when the regional arrival time is fixed to a constant value instead of being estimated for each pixel.

Simulated and measured PET data consistently demonstrate that much of the bias introduced into the CBF values by arterial blood contamination can be effectively eliminated by exclusion of the early PET data, which contain high arterial radiotracer concentrations. In the results presented in this paper, 40 sec of data were excluded because the PET data was acquired as 20 sec scans. Therefore, only exclusions that were multiples of 20 sec could be tested with actual PET data. Results strongly indicate that exclusion of 40 sec of data is superior to exclusion of either 20 sec or 60 sec of data. If the PET data were acquired on a finer time grid, more intermediate values could be tested, how-

ever, the processing time and data storage requirements increase as the number of scans acquired in the dynamic sequence increases.

Figure 2 shows that the effect of arterial blood contributing to the measured PET signal begins to significantly affect CBF estimates when the arterial blood fraction reaches ~2%. At this level, overestimations of CBF can range from 10% to 15%. There is some flow dependence to this error with regions of lower flow having increased error for the same arterial blood fraction. When the first 40 sec of data are omitted from the estimation calculations, a 2% arterial blood fraction causes overestimations in CBF of only 1%–3%.

This effect is easily visible in the areas surrounding the carotid arteries, as shown in Figure 3. The mean CBF value of the regions around the carotid arteries, shown in Figure 4, decreased from 60.2 to 31.7 ml/100 ml/min when the first 40 sec of data are excluded. The effect is also noticeable in areas with high cerebral blood volume, such as the temporal lobe regions where the mean CBF value decreased from 63.6 to 57.5 ml/100 ml/min. CBF estimates using a dynamic analysis were higher by an average of over 50% in regions surrounding the carotid arteries when all the data were included. Similarly, gray matter region estimates typically increased by 6%–8%, whereas, white matter region estimates increased by only 2%–3%. This occurs because there are two parameters that co-vary, one parameter (f) adjusts to fit the early data that has blood contamination and the second (p) adjusts to fit the remainder of the data. The sensitivity of the single scan method to the early data was found to vary considerably with scan duration. If only a short interval of data was used, the single scan method is equally or more sensitive to arterial effects than the dynamic method. Increases in flow values of up to 60% in areas near major arteries and 6%–7% in gray matter regions were seen when the first 40 sec of data were included. As progressively longer scans were used, the bias from arterial-borne radioactivity decreased because the fraction of the data that had a significant contribution from blood-borne radioactivity was decreasing. However, longer scan durations for the single scan techniques become more sensitive to other types of errors, such as bias encountered when using an incorrectly fixed tissue-blood partition coefficient (*11*).

The two major limitations of performing this type of correction are that (a) the first 40 sec of data also contains the most useful flow information, and (b) statistical requirements limit the amount of data that can be omitted from the CBF estimations. For dynamic studies, the biases due to a 1.5% arterial blood volume are decreased from 5%–10% to <1% by omitting the first 40 sec of data. However, exclusion of the early data increases the percent root-mean-squared uncertainty in estimated CBF from ~5% to ~8%. Therefore, part of the gain in accuracy obtained by removing the arterial bias is lost as the CBF estimates become less precise.

Other methods of correction for CBV contamination appear less promising. Estimation of arterial CBV as an additional model parameter is difficult in dynamic studies due to the noise characteristics of PET data, and is not even possible in static studies because only a single parameter can be estimated. Another means of correcting for arterial blood volume would be to measure CBV with an additional PET study. However, this requires extra scanning time and often presents registration problems. Furthermore, the magnitude of the biases does not seem to warrant taking an additional scan when most of the error can be avoided by omitting approximately the first 40 sec of data from the CBF calculations.

Variations in the actual arrival time of the arterial bolus of ±3 sec from the mean arterial arrival time were predicted by computer simulations to cause up to 12% bias in estimated CBF values (Table 3). Results for the autoradiographic methods are in good agreement with those reported previously (*12,19*). In addition, dynamic and short single scan protocols have greater biases than do longer single scan protocols. As is the case with CBV errors, omission of the early data decreases biases in estimated CBF. Biases in the dynamic studies are reduced to <1.5%, while biases in static scans shorter than 2 min are reduced to <2.5% when the first 40 sec of data are excluded. In general, if the actual arrival time is longer than the mean arrival time (positive time shifts), biases in CBF are positive. One major exception is that for the longer static studies this error reverses and longer arrival times cause negative biases in CBF. This is understood by considering how the integral of the PET data changes as the limits of integration change. A positive time shift causes both the starting and ending limit to move later in time. Thus, when the scan duration is short and includes data immediately following tracer administration, the integral becomes larger because early time points that are at low concentrations are replaced by later time points that are at higher concentrations. As the scan duration increases, or when early data are omitted, the integral does not change as rapidly and biases due to timing errors become less significant. Shifts of the measured input function are seen to create changes in estimated CBF that are in good agreement with those predicted by theoretical calculations.

Inclusion of arrival time as an additional fitted model parameter indicates that arrival of the arterial bolus differs by several seconds between brain regions (Table 4). For example, arrival times near the carotid arteries were consistently earlier, and arrival times in the cerebellum and white matter were consistently later than those of cortical gray matter, with variations of up to several seconds. However, fitting arrival time as an

additional model parameter has limitations because of the extra computational time required in a dynamic analysis and because it can not be implemented in static methods. Furthermore, while bias is reduced by including a variable time shift into the model, the statistical variation in the estimates of the other parameters (blood flow and partition coefficient) will increase due to the additional degree of freedom allowed in the fitting process. As is the case with arterial blood contamination problems, most of the error can be avoided by omitting approximately the first 40 sec of data from the CBF calculation.

The assumptions investigated in this paper are only two of several made in PET CBF measurements. Many groups have examined errors in blood flow estimates resulting from statistical uncertainty in the PET measurements as well as biases introduced by failure of various model assumptions (*3,11–19,21*). Statistical uncertainty in PET blood flow values is typically 5%–10%. The magnitude of the biases discussed here range from a few percent to >20% depending on the particular conditions, and thus are potentially a larger source of error than statistical uncertainty. These biases are also as or more significant than biases caused by other previously examined assumptions, such as tissue imhomogeneities, input function dispersion, and incorrect values for the partition coefficient, which seldom cause biases >10%–15%.

In conclusion, we have examined in detail two of the more common assumptions made in PET cerebral blood flow techniques. Biases in estimated CBF values, when these assumptions fail to be completely valid, were quantitated for both dynamic and single scan PET methods. Both theoretical computer simulation studies and measured PET data indicate that these biases can be significant under normal scanning conditions, particularly in regions near the major arteries. Omission of the early data following tracer administration (~40 sec) from the estimation calculations has been shown to considerably lessen the magnitude of the biases associated with these sources of error.

ACKNOWLEDGMENTS

This work was supported in part by the National Institutes of Health grant number P01-NS15655 awarded by NINCDS. The authors thank the Cyclotron/P.E.T. Facility staff for production of radiopharmaceuticals and for acquisition of PET data reported in this work.

REFERENCES

1. Huang S-C, Carson RE, Hoffman EJ, et al. Quantitative measurement of local cerebral blood flow in humans by positron computed tomography and ^{15}O-water. *J Cereb Blood Flow Metab* 1983; 3:141–153.
2. Ginsberg MD, Lockwood AH, Busto R, et al. A simplified *in vivo* autoradiographic strategy for the determination of regional cerebral blood flow by positron emission tomography: theoretical considerations and validation studies in rats. *J Cereb Blood Flow Metab* 1982; 2:89–98.
3. Raichle ME, Martin WRW, Herscovitch P, et al. Brain blood flow measured with intravenous $H_2{}^{15}O$. 2. Implementation and validation. *J Nucl Med* 1983; 24:790–798.
4. Subranamyam R, Alpert NM, Hoop B, et al. A model for regional cerebral oxygen distribution during continuous inhalation of $^{15}O_2$, $C^{15}O$, and $C^{15}O_2$. *J Nucl Med* 1978; 19:48–53.
5. Frackowiak RSJ, Lenzi G-L, Jones T, et al. Quantitative measurement of regional cerebral blood flow and oxygen metabolism in man using ^{15}O and positron emission tomography: theory, procedure, and normal values. *J Comput Assist Tomogr* 1980; 4:727–736.
6. Holden JE, Gatley SJ, Nickles RJ, et al. Regional cerebral blood flow with fluoromethane and positron emission tomography. In: Positron emission tomography of the brain. Berlin: Springer-Verlag, 1983: 90–94.
7. Koeppe RA, Holden JE, Polcyn RE, et al. Quantitation of local cerebral blood flow and partition coefficient without arterial sampling: theory and validation. *J Cereb Blood Flow Metabol* 1985; 5:214–224.
8. Herscovitch P, Raichle ME, Kilbourn MR, et al. Measurement of cerebral blood flow and water permeability with positron emission tomography using O-15 water and C-11 butanol. *J Cereb Blood Flow Metab* 1985; 5 (suppl 1):567–568.
9. Takahashi K, Murikami M, Hagami E, et al. Radiosynthesis of ^{15}O-labeled butanol available for clinical use. In: Proceedings of the Sixth International Symposium on Radiopharmaceutical Chemistry. 1986: 81–82.
10. Yamamoto YL, Thompson CJ, Meyer E, et al. Dynamic positron emission tomography for the study of cerebral hemodynamics in a cross section of the head using positron emitting ^{68}Ga-EDTA and ^{77}Kr. *J Comput Assist Tomogr* 1977; 1:43–56.
11. Hutchins GD, Koeppe RA, Hichwa RD, et al. The effect of partition coefficient values for water on the estimation of lCBF and $lCMRO_2$ in PET. *J Nucl Med* 1986; 27:941.
12. Iida H, Kanno I, Miura S, et al. Error analysis of a quantitative cerebral blood flow measurement using $H_2{}^{15}O$ autoradiography and positron emission tomography, with respect to the dispersion of the input function. *J Cereb Blood Flow Metab* 1986; 6:536–545.
13. Huang S-C, Gamhbir SS, Hawkins RA, et al. Investigation of Kety-Schmidt single-compartment model for O-15 water in CBF measurements using PET. *J Nucl Med* 1986; 27:913.
14. Herscovitch P, Raichle ME. Effect of tissue heterogeneity on the measurement of cerebral blood flow with the equilibrium $C^{15}O_2$ inhalation technique. *J Cereb Blood Flow Metab* 1983; 3:407–415.
15. Koeppe RA, Holden JE, Ip WR. Performance comparison of parameter estimation techniques for the quantitation of local cerebral blood flow by dynamic positron emission tomography. *J Cereb Blood Flow Metab* 1985; 5:224–234.
16. Huang S-C, Carson RE, Phelps ME. Measurement of local blood flow and distribution volume with short-lived isotopes: a general input technique. *J Cereb*

Blood Flow Metab 1982; 2:99–108.
17. Carson RE, Huang S-C, Green MV. Weighted integration method for local cerebral blood flow measurements with positron emission tomography. *J Cereb Blood Flow Metab* 1986; 6:245–258.
18. Alpert NM, Eriksson L, Chang JY, et al. Strategy for the measurement of regional cerebral blood flow using short-lived tracers and emission tomography. *J Cereb Blood Flow Metab* 1984; 4:28–34.
19. Herscovitch P, Markham J, Raichle ME. Brain blood flow measured with intravenous $H_2{}^{15}O$. Theory and error analysis. *J Nucl Med* 1983; 24:782–789.
20. Hutchins GD, Hichwa RD, Koeppe RA. A continuous flow input function detector of $H_2{}^{15}O$ blood flow studies in positron emission tomography. *IEEE Trans Nucl Sci* 1986; 33:546–549.
21. Ginsberg MD, Howard BE, Hassel WR. Emission tomographic measurement of local cerebral blood flow in humans by an *in vivo* autoradiographic strategy. *Ann Neurol* 1984; 15 (suppl):S12–S18.